

## INTEGRATED THERMAL ANALYSIS OF THE PRODUCTION DIPOLE MAGNETS FOR THE SUPERCONDUCTING SUPER COLLIDER

G.E. Hardy, S.D. Peck  
General Dynamics Space Systems Division  
P.O. Box 85990, San Diego, CA 92138

### Abstract

A thermal model of a 16.6-meter-long Superconducting Super Collider dipole cryostat was developed to understand the system thermal behavior of the dipoles. The model incorporates in detail all the heat flow paths in the cryostat, with the capacity to model all steady-state and transient thermal boundary conditions to which the cryostat is subjected during normal and upset conditions. The model predicts heat leaks to the cryogenics of 25.4 watts per dipole to 80K, 2.64 watts per dipole to 20K, and 0.174 watts per dipole to 4.35K during normal operation, which compare favorably to the established heat leak budgets. The 4.35K value does not include synchrotron radiation. The heat leak to the cold mass is below the budget at a vacuum of  $10^{-5}$  torr, but rapidly exceeds the budget as the pressure increases. However, with ten layers of MLI on the cold mass, the budget value is met even at  $10^{-5}$  torr. The heat leak in the cryostat is shown to be sensitive to the gas pressure, the inner shield temperature and the MLI thickness but not to the thermal shield thickness, the thermal shield weld frequency, or the emissivity of the vacuum vessel or shield.

The model shows that the synchrotron radiation does not raise the temperature of the winding more than 0.2K relative to the inlet temperature of the helium. Cooldown from room temperature to 55K is shown to take from 1.5 to 3 hours with flow rates of the order of 100-200 g/sec. Warmup to room temperature from steady-state operating conditions takes approximately 17.5 hours using two 5 kW heaters. Re-cooling of the winding following a quench takes about 3.5 minutes from 70K and 9 minutes from 300K. The heat rate to the helium in the yoke cooling channels ramps to 0.57 kW/m in 45 seconds with the windings initially at 70K. This heat rate changes to 3.6 kW/m 2 minutes after quench for an initial winding temperature of 300K.

### Introduction

The thermal performance of the cryostats for the dipoles of the SSC has a large impact on several aspects of the capital and operating costs of the accelerator. The function of the cryostat is to create a structural and thermal environment that provides accurate and precise placement of the magnetic field, with provision for rapid changeout of defective magnets to minimize accelerator downtime, allows the superconducting magnet to safely transition from room temperature to operating temperature and back, and maintains the operating temperature of the superconductor below the critical temperature while limiting the refrigeration requirements to acceptable levels.

The capital costs are affected by the amount of insulating material and/or special manufacturing techniques used to limit the heat leak, and by the size of the refrigeration plant required for the ring. The operating costs also depend on the size of the heat leak. Operating costs are also affected by the down time required for maintenance on the magnets. One would like to minimize this time, which means that the cryostat should be designed to be forgiving of upset conditions, such as a magnet quench, and of poor performance of other subsystems, such as the vacuum system. The cryostat should also be capable of rapid warmup, replacement, and rapid cooldown in cases where the magnet becomes inoperable.

The objective of this study is twofold: first, to develop a tool to address the above issues analytically; and second, to understand the system thermal behavior of the SSC dipoles. A thermal model of an SSC dipole cryostat and cold mass was built to do this. The goal is to quantify the thermal behavior of the baseline design, and to learn how sensitive it is to changes in design or operating parameters.

### Description Of Models

Three different models were built to look at the different aspects of the SSC thermal behavior. For the steady-state conditions, a two-dimensional model of a cross-section of the cryostat at a support post location was used. Cooldown and warmup transients were modeled in

three dimensions, by extending the two-d model to cover the entire length of the cryostat. A very detailed two-d model of the cold mass was used to look at temperature gradients in the cold mass. All heat transfer paths, fluid flows, and potential energy inputs were included in the models. Various boundary and initial conditions were imposed to simulate different operating and upset conditions.

### Cryostat/Cold Mass Modeling

The integrated thermal math model (ITMM) of the SSC dipole incorporates performance data and geometric descriptions of the thermal control elements of one dipole cryostat without connecting regions. The elements included in the model are shown in Figure 1. The SSC dipole is modeled by seven sections along its length (axial direction), five sections with support posts, and two without. This sectional modeling allows for the development of separate models for steady-state and transient analyses. For steady-state cases, a single section with support post was analyzed. For transient cases, a complete seven-section model was used. Figure 2 shows the axial modeling of the SSC dipole.

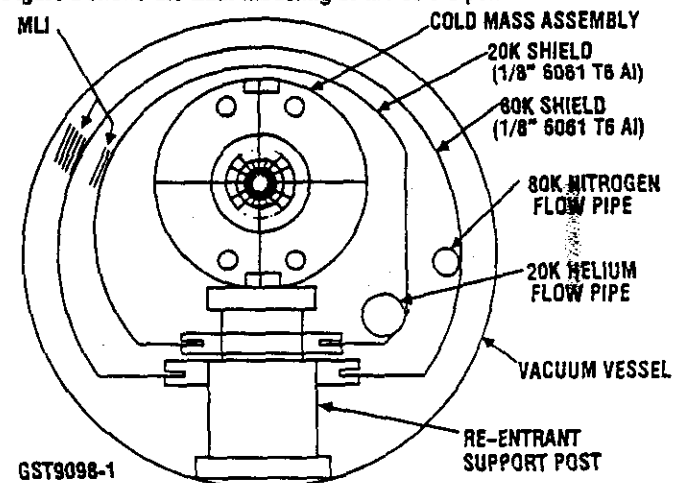


Figure 1. SSC cryostat showing coldmass, heat shields, flow channels, support post, and vacuum vessel.

### Analytical Method

The models were solved using the Convair Thermal Analyzer code P4560E.<sup>1</sup> The Thermal Analyzer is a lumped parameter heat transfer code, in which node temperatures are determined by solving an energy balance equation at each node. Fluid flow can also be simulated by means of strings of fluid flow nodes, which honor the energy balance equation for a fully developed, steady, one-dimensional, incompressible flow. Fluid flow nodes are used in the ITMM to represent the liquid nitrogen coolant in the 80K shield, the helium gas in the 20K shield, and the supercritical helium flowing in the four large cooling passages and in the annulus surrounding the beam tube in the cold mass.

The Thermal Analyzer employs a Crank-Nicholson difference representation of the temperature time derivatives, and uses Gauss-Seidel over-relaxation to solve the set of simultaneous non-linear equations resulting from applying node energy balances throughout the model.

### Steady-State Boundary Conditions

The steady-state boundary conditions imposed on the models fall into three categories: flow rates and cryogen inlet temperatures, heat inputs imposed on various components for various operating conditions, and fixed boundary temperatures.<sup>2</sup>

**Flow** — The total helium flow to the cold mass for all steady-state cases is 100 g/s. The 20K thermal shield helium flow rate is also 100 g/s. The nominal steady-state flow rate for LN<sub>2</sub> in the 80K thermal shield is 750 g/s. The helium flow inlet temperature is constrained to 4K in the cold mass and 20K in the 20K thermal shield. The LN<sub>2</sub> inlet temperature is set to 80K in the 80K thermal shield.<sup>2</sup>

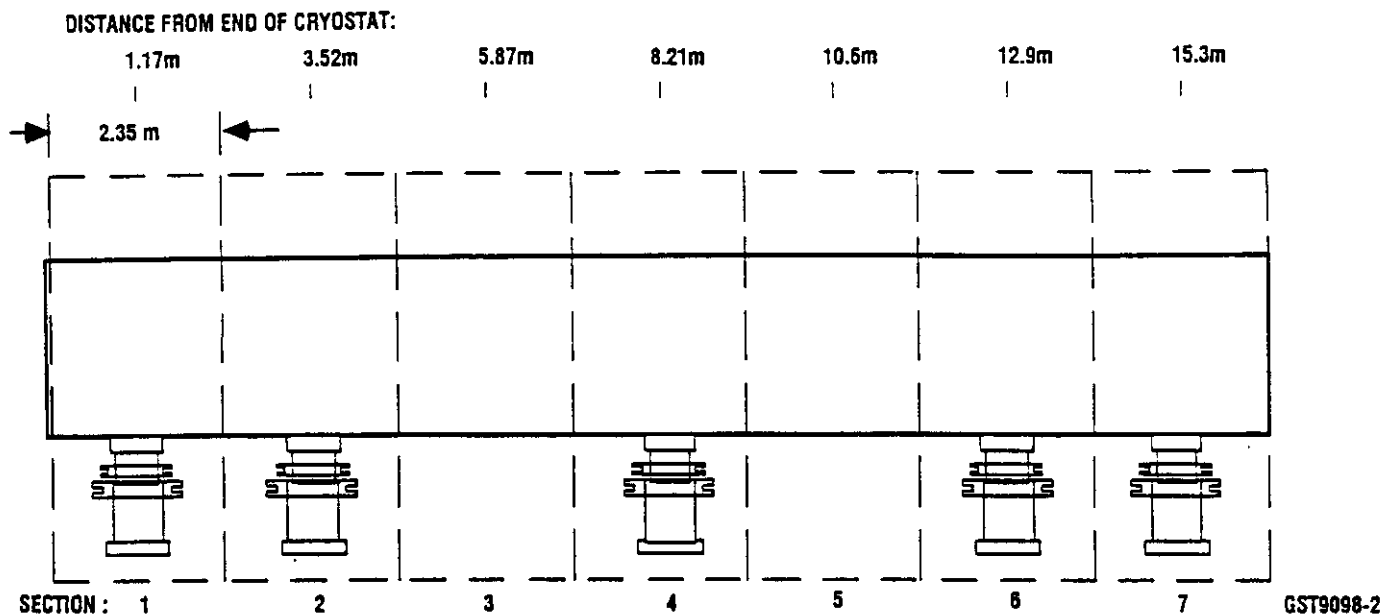


Figure 2. SSC section numbering and axial nodal division.

The flow split among the cold mass flow passages is determined by requiring the pressure drop along each passage to be equal. The friction factor is determined iteratively as a function of the Reynolds number in the passage. A Moody diagram is used, and surface roughness of the passage walls is considered. It is estimated that the laminations form a 0.0025 cm "bump," which is used to calculate the surface roughness. The calculations converge for a flow split of 98.9% to the four yoke cooling channels, with a Reynolds number of 278000; 1.1% to the annulus around the beam tube, with a Reynolds number of 9700; and 0.02% to the gap between the collar and yoke, with a Reynolds number of about 300.

**Heat Inputs** — The only steady-state heat input imposed on the model is the synchrotron radiation that heats the beam tube. The synchrotron radiation to the beam tube is 0.14 watts/meter (2.38 watts per dipole).<sup>3</sup>

**Fixed Temperatures** — The only fixed boundary temperature in the model aside from the flow inlet temperatures is the environmental temperature outside the vacuum vessel. This temperature is fixed at 300K and the vacuum vessel communicates with this environment via a free convection heat transfer coefficient.

#### Transient Boundary Conditions

The transient boundary conditions again fall into the three categories mentioned for the steady-state conditions. Initial conditions are required for cooldown, warmup and cooldown following a quench.

**Cooldown** — Two cooldown scenarios were examined. In either case the cooldown proceeds from room temperature to 55K. This is the temperature range of interest because most of the thermal contraction occurs above 55K, and most of the sensible heat of the system is stored above 55K. The first scenario is a normal cooldown of the ring. For this scenario, a helium flow rate of 93 g/sec to the cold mass is specified, with 7 g/sec going to the 20K shield.<sup>2</sup> The second scenario is a rapid cooldown of a half-cell. In this case the flow rate of helium to the cold mass is 200 g/sec, with 200 g/sec going to the 20K shield as well.<sup>4</sup> In both cooldown cases the initial temperature throughout the cryostat is 300K and the inlet temperature of the helium flow to both the cold mass and shield is 55K.

The 80K thermal shield flow rate was 61 g/sec of nitrogen gas with an inlet temperature of 80K for both cooldown cases analyzed. The value of 61 g/sec is determined arbitrarily by scaling the flow rate such that the pressure drop during cooldown is the same as the pressure drop during normal operation. This is an arbitrary choice, not expected to reflect the real situation.

**Warmup** — The initial condition for the warmup analysis is the steady-state operating temperatures for the cryostat (i.e., cold mass at 4K). The flow is set to zero in the cold mass and shields, and two 5 kW

heaters running the length of the cold mass are turned on in the yoke.<sup>4</sup> This case was run until the cold mass reached room temperature.

**Post-Quench** — The ITMM does not have the necessary detail to accurately analyze a quench of a magnet, nor does the Thermal Analyzer have the capability to model the complex flow processes that occur during a quench. However, some useful information about the time period immediately following the decay of the current in the winding may be obtained from the ITMM. The initial temperatures for the post-quench winding behavior study are determined by simulating an energy deposit equal to the total stored energy of 1.06 MJ into various lengths of magnet, thus simulating the effect of different initial normal zone lengths. The stored magnetic energy is dissipated in the winding which produces a temperature rise to 70K, 80K, 95K, 120K, or 300K corresponding to normal zone lengths of 24.4m, 16.6m, 10.79m, 6.31m, 1.28m. This heat then diffuses through the cold mass structure into the helium in the yoke cooling channels. It is assumed that the helium remains at 4K while absorbing the quench energy. This is conservative in that the power to the helium is overestimated. For the post quench analysis the winding nodes are initialized to 70K, 80K, 95K, 120K, or 300K while the rest of the cold mass is at 4K. The helium flow in the beam tube flow channel and the collar/yoke flow channel are not modeled, as it is assumed that these channels do not provide any significant cooling. The four-yoke helium flow channel nodes are constrained to 4K, irrespective of any flow that is occurring.

#### Steady-State Results

**Temperature Of Winding** — The stability margin of the magnet depends on the temperature rise of the helium in the beam tube channel due to the synchrotron radiation. The model predicts a helium temperature rise of less than 0.2K for a heating level of 0.14 W/m. This result from the computer model was compared to an analytical model of an energy balance on the helium in the beam tube annulus:

$$m c_p \frac{dT_{He}}{dx} = q'_{rad} - U' (T_{He} - T_b) \quad (1)$$

where  $m$  = flow rate in the beam tube annulus,  
 $c_p$  = specific heat of the helium,  
 $T_{He}$  = the local temperature of the helium in the annulus,  
 $q'_{rad}$  = synchrotron heat rate per unit length,  
 $U'$  = effective thermal conductance per unit length between the beam tube annulus and the helium in the yoke cooling channels,  
and  $T_b$  = the helium temperature in the yoke cooling channels (assumed constant).

The solution to (1) becomes independent of length after a few meters, so that at the end of a dipole, the temperature rise of the helium in the beam tube, relative to that in the yoke, is given by  $\Delta T = q'_{rad}/U'$ . The calculated temperature rise is sensitive to the value used for the

thermal conductance between channels. The value in the ITMM is 0.814 W/K-m, which yields a  $\Delta T$  of 0.172K. This value of  $U'$  accounts for the parallel heat flow paths through the collar and winding to the yoke and thence to the cooling channels.

A comparison between the budget temperature drop (0.055K) in the cold mass and the temperature drop predicted in this analysis (0.172K) is illustrated in Figure 3.<sup>2</sup> The major difference between the two is across the Kapton. This is due to the Kapton thermal conductivity used in this analysis.<sup>5</sup> If a ten times higher value of Kapton thermal conductivity is used (a roughly ten times higher value was used in developing the budget value) then the temperature drop in the cold mass is predicted to be approximately 0.067K (Figure 3). More Kapton is modeled in this analysis than in the budget analysis (0.04 cm), which could explain the slight temperature drop difference between this analysis and the budget values (0.067K vs 0.055K).

The temperature drops obtained by relying only on conduction through the winding are too high for reliable operation of the coil, especially when the major thermal resistance, the Kapton insulation, is not well known. Fortunately, an alternate heat transfer mechanism exists within the cold mass. That is the convection of the helium in the gaps between subassemblies of collar and yoke laminations. This mechanism was modeled to see if it was capable of passing the synchrotron heating through the winding at acceptable temperatures.

A parametric study was performed by varying the heat transfer coefficient  $h$  between the collar/yoke annular gap and the inner surface of the windings. The value of  $h$  was varied from  $6 \times 10^{-6}$  to  $1 \times 10^{-1}$  W/cm<sup>2</sup>K. This range was used to establish the sensitivity of the temperature drop to the heat transfer coefficient. Figure 4 shows the temperature difference in the cold mass versus  $h$ . In the free convection regime ( $h = 3 \times 10^{-2}$  w/cm<sup>2</sup>K) shown on Figure 4, the temperature difference in the cold mass is 0.10 K. A heat transfer coefficient on the order of  $1 \times 10^{-1}$  is necessary to bring the temperature drop in the cold mass below the CDG budget of 0.055K. The Rayleigh number developed was in a transition region for laminar and turbulent convection.<sup>6</sup> The laminar correlations were used for conservatism. Turbulent flow correlations would improve the

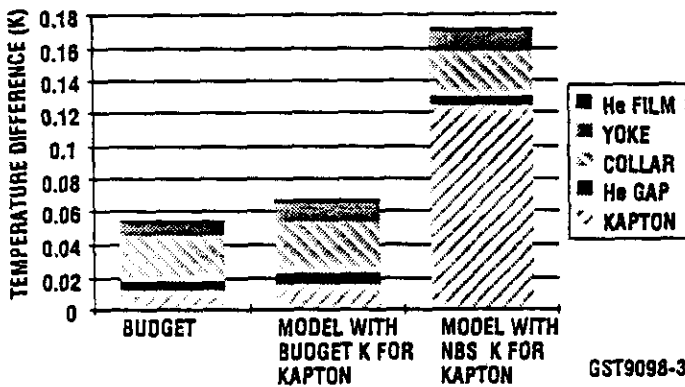


Figure 3. Steady-state temperature difference in the cold mass is very sensitive to the thermal resistance of Kapton.

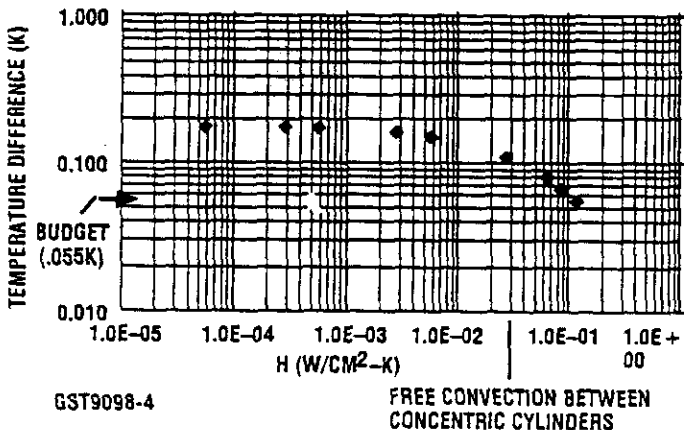


Figure 4. Temperature difference in cold mass versus heat transfer coefficient in lamination gaps in collar and yoke.

heat transfer in the collar/yoke lamination gaps. By accounting for convective heat transfer in the lamination gaps, the Kapton thermal conductivity issue becomes mute.

**Heat Leak vs Gas Pressure** — Although the nominal vacuum level in the cryostat is  $10^{-8}$  torr, the realities of collider operation require the SSC to be operable with considerably poorer vacuum. The various heat leaks are determined at different pressure levels to quantify the relationship between pressure and heat leak. The heat leak to the 80K thermal shield is not very sensitive to the gas pressure since radiation and conduction through the spacer material in the MLI blankets dominate the heat transfer in this region (see Figure 5). The heat leak to the 20K thermal shield starts increasing substantially above  $10^{-5}$  torr (see Figure 5). The area of greatest concern for pressure changes is the 4K cold mass where gaseous conduction can dominate radiation (and spacer conduction if a blanket is present). Figure 5 demonstrates the effect of having a ten-layer MLI blanket on the cold mass. This region is highly sensitive to pressure and the presence of the MLI reduces the heat leak to the cold mass noticeably at pressures above 10 torr. At  $8 \times 10^{-5}$  torr, the 20K shield starts putting heat into the cold mass if the gas inlet temperature is constrained to 20K.

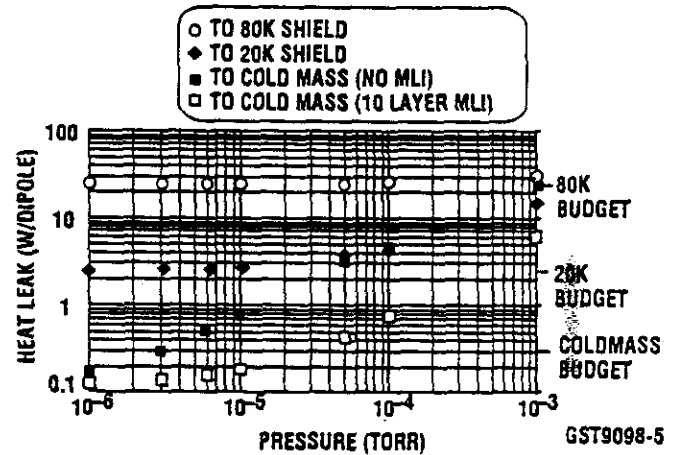


Figure 5. Heat leak versus gas pressure for SSC ITMM trade study.

**Heat Leak vs MLI Thickness** — MLI is effective in reducing the heat leak to a cryogen, but only if the capital cost of the MLI is less than the "cost" of refrigeration the MLI saves. The heat leak to the 80K shield can be reduced 23% from 25.4W to 19.6W by increasing the number of MLI layers from 64 to 96. The 20K shield heat leak can be decreased 12% from 2.64W to 2.33W by increasing the number of layers from 16 to 24. The presence of a ten-layer MLI blanket on the cold mass decreases the heat leak to the cold mass by 31% from 0.174W to 0.12W.

**Heat Leak vs Shield Temperature** — The outer shield heat leak is insensitive to the inner shield temperature. The heat leak varies from 24.2W to 26.3W with the outer shield at 70K to 90K, indicating a slight sensitivity to the outer shield temperature. The heat leak budget for the outer shield (25 W/dipole) is exceeded with the outer shield at 70K and 80K. With the outer shield at 90K the heat leak is under budget at 24.2 W/dipole.

The inner shield heat leak is slightly sensitive to its own temperature, showing a 0.4 W/dipole variation from 10K to 30K (15% decrease). The heat leak varies 1.7 W/dipole for the outer shield at 70K to 90K (90% increase), indicating a strong sensitivity to the outer shield temperature. The heat leak budget for the inner shield (2.5 W/dipole) is exceeded with the outer shield at 80K and 90K. With the outer shield at 70K the heat leak is under budget at 2.0W/dipole or less.

The cold mass heat leak is insensitive to the outer shield temperature, showing no variation in heat leak. The heat leak varies 0.29 W/dipole with the inner shield at 10K to 30K, indicating a strong sensitivity to the inner shield temperature (461% increase). The heat leak budget for the cold mass (0.3 W/dipole) is exceeded with the inner shield at temperatures higher than 25K.

At the design point (i.e., inner shield at 20K, outer shield at 80K,  $p = 1 \times 10^{-8}$  torr) the predicted heat leaks compare favorably with Fermi Lab measurements.<sup>7</sup>

### Transient Results

**Cooldown From Room Temperature** — The cold mass cools down to 55K in approximately 3 hours with a 93 g/s flow rate. The axial temperature distributions vs time in the winding are shown in Figure 6, for the baseline case of a stainless steel collar. Figure 7 shows the radial temperature distribution vs time at the inlet of the magnet where the greatest axial temperature distribution exists.

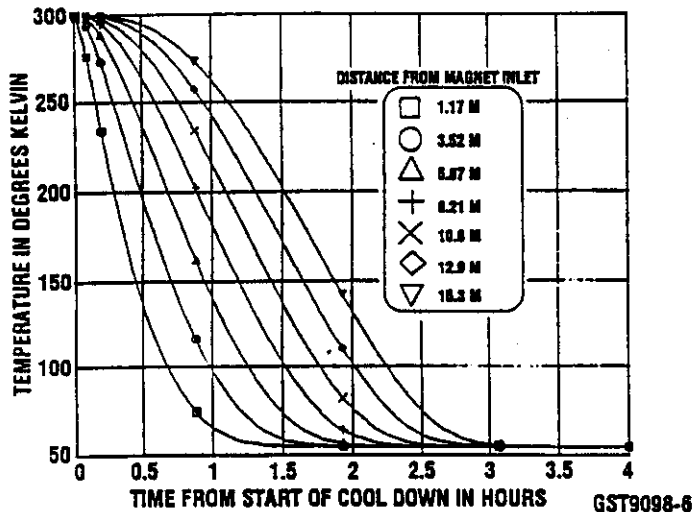


Figure 6. Winding temperatures along cryostat during cooldown (93 g/sec flow, stainless steel collar).

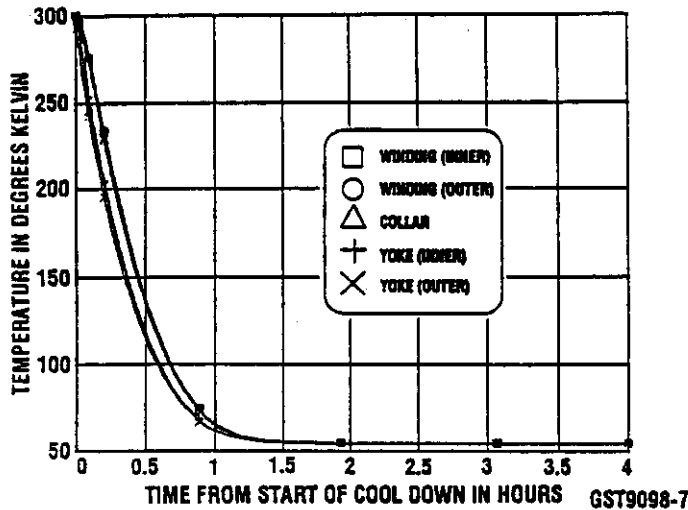


Figure 7. Cold mass temperatures at inlet section during cooldown (93 g/sec flow, stainless steel collar).

The second cooldown case analyzed is at 200 g/s flowrate to the cold mass. In this case cooldown to 55K occurs in approximately 1.5 hours.

**Warmup** — The warmup from steady-state operating temperature to room temperature takes approximately 17.5 hours when the heaters dissipate a total of 10 kW per dipole. No substantial temperature gradient occurs in the cold mass during the warmup.

**Post-Quench** — With the winding initially at 70K the heating rate to the helium in the yoke channels ramps to about 0.57 kW/m in 45 seconds, then ramps back down to zero after an additional 135 seconds.

The heating occurs over a length of 24.4m, which demonstrates a normal zone of greater than one magnet (16.6m). With the winding initially at 80K the power ramps to 0.75 kW/m in 50 seconds, then ramps back down to zero after an additional 190 seconds. In this case the heating occurs over one magnet length of 16.6m. For the case where the winding is initially at 95K the power ramps to about 1.02 kW/m (over 10.8m) in 50 seconds, then ramps back down to zero after an additional 220 seconds. With the winding initially at 120K the peak power is 1.45kW/m spread over 6.31m at 50 seconds and ramps back down to essentially zero after an additional 280 seconds. With the winding initially at 300K the power ramps to about 3.55 kW/m (over 1.28m) in 2 minutes then ramps back down to zero after an additional 7 minutes. Figure 8 summarizes the post-quench study showing the normal zone length, initial temperature, peak heat rate, and cooldown time for all cases.

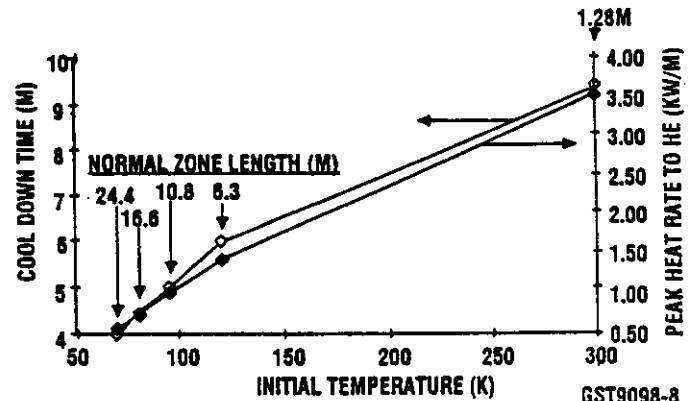


Figure 8. Summary of post-quench study showing normal zone length, initial temperature, peak heat rate, and cooldown time.

Work supported by Universities Research Association under U.S. Department of Energy Contract Number DE-AC02-76CH03000-01.

### References

- [1] "Thermal Analyzer Engineering Manual and User's Guide," Report GDSS-SP-85-012, December 15, 1985.
- [2] SSC Central Design Group, "Conceptual Design of the Superconducting Super Collider," Report SSC-SR-2020, March 1986.
- [3] Jackson, J.D., "Conduction of Heat of Synchrotron Radiation Through the Wrapped Beam Tube Wall," Report SSC-N-235, September 1986.
- [4] Personal communication with V. Karpenko, Central Design Group, Lawrence Berkeley Laboratory.
- [5] Radebaugh, Frederick, Siegworth "Kapton Thermal Conductivity," (NBS 132) 1972.
- [6] Raithby, G.D. and K.G.T. Hollands, "A General Method of Obtaining Approximate Solutions to Laminar and Turbulent Free Convection Problems," in T.F. Irvine & J.P. Hartnett, eds., *Advances in Heat Transfer*, Vol.II, Academic Press, New York, 1975, pp 265-315.
- [7] Niemann, R.C., et al., "SSC Dipole Cryostat Thermal Model Measurement Results," in *Advances in Cryogenic Engineering*, Vol. 33, Plenum Press, New York (1988), p. 251.